Synthesis and Reactions of Monomeric Hydrazine and Hydrazido Complexes That Contain the Cp^*MoMe_3 Core

Michael G. Vale and Richard R. Schrock*

Department of Chemistry, 6-331, Massachusetts Institute of Technology, Cambridge, Massachusetts 02139

Received December 16, 1992

Addition of N_2H_4, N_2H_3Me, NH_2NMe_2, or NHMeNHMe to $Cp^*MoMe_3(OTf)$ yields complexes of the type $[Cp^*MoMe_3(N_2H_xMe_y)]OTf$. Attempted deprotonation of cationic Mo(V) adducts that contain methylhydrazine or 1,1-dimethylhydrazine yields $Cp^*MoMe_3(NNMeH)$ and $Cp^*MoMe_3(NNMe_2)$ in ca. 50% yield, but attempted deprotonation of $[Cp^*MoMe_3(NH_2NH_2)]OTf$ yields no recognizable products. Hydrazido(2–) complexes also can be prepared by adding methylhydrazine or 1,1-dimethylhydrazine to $[Cp^*MoMe_3(OAr)]PF_6$. $Cp^*MoMe_3(NNMeH)$ reacts with butyllithium to give $Cp^*MoMe_3(NNMeLi)$, a yellow-orange crystalline solid that decomposes in the solid state in a matter of hours. Addition of triethylamine to $[Cp^*MoMe_3(NHMeNHMe)]OTf$ gives $[Cp^*MoMe_3(NMeNMeH)]OTf$ in ca. 50% yield. Addition of HX (X = Cl, OTf, BF_4, $B[3,5\text{-}C_6H_3(CF_3)_2]_4$) to $Cp^*MoMe_3(NNRR')$ complexes (R = Me; R' = H, Me) yields $Cp^*MoMe_2X(NNRR')$ complexes. Methyl triflate reacts with $Cp^*MoMe_3(NNMe_2)$ to yield $[Cp^*MoMe_3(NNMe_3)]^+$, which was shown in an X-ray study to be approximately a square pyramid with a Mo–N(1) bond distance of 1.735(4) Å and a Mo–N(1)–N(2) angle of 179.2(3)°. (Space group = $P2_1/c$, a = 9.173(1) Å, b = 8.724(3) Å, c = 32.091(6) Å, β = 91.56(2)°, V = 2567(1) Å^3, MW = 583.39, ρ(calcd) = 1.509 g/cm^3, Z = 4, and μ = 8.28 cm^{-1}.) $[Cp^*MoMe_3(NH_2NH_2)]^+$ is reduced by zinc amalgam in the presence of 2,6-lutidine hydrochloride to give 1.84 equiv of ammonia. $[Cp^*MoMe_3(NH_2NH_2)]^+$ also is a catalyst for the reduction of hydrazine to ammonia under similar conditions. Although decomposition reactions that involve loss of a methyl group in part complicate the chemistry of Cp^*MoMe_3 relative to that of Cp^*WMe_3, controlled cleavage of the N–N bond and catalytic reduction of hydrazine in the Mo system suggest that there is no significant difference between Mo and W as far as reduction of the N–N bond beyond the hydrazido(2–) stage is concerned.

Introduction

Steps that are relevant to the reduction of dinitrogen at a metal center in a relatively high oxidation state have been explored in our laboratory over the last few years in the form of chemistry of complexes that contain the Cp^*WMe_3 core. For example, $[Cp^*WMe_3]_2(\mu\text{-}N_2)$ can be prepared in high yield by reducing $Cp^*WMe_3(OTf)$ (Cp^* = η^5-C_5Me_5, OTf = OSO_2CF_3) in the presence of dinitrogen,[1] good evidence that dinitrogen can bind to a metal in a relatively high oxidation state (probably W(4+) in this case, i.e., Cp^*WMe_3). Many monomeric N_2H_x species (x = 2–4) that contain the Cp^*WMe_3 core also are now known, examples being $[Cp^*WMe_3(\eta^2\text{-}NHNH_2)]^+$ [2] and $[Cp^*WMe_3(\eta^2\text{-}NH_2NH_2)]^+$,[3,4] as well as complexes containing NH_y ligands that are possible intermediates in a reduction cycle, e.g., $Cp^*WMe_3(NH)$, $Cp^*WMe_3(NH_2)$, and $[Cp^*WMe_3(NH_3)_x]^+$ (x = 1, 2).[5] We have found that ammonia is produced in high yield when monomeric Cp^*WMe_3 species in which the N–N bond is still present are reduced in the presence of protons[3,4] and that hydrazine can be reduced catalytically to ammonia under similar conditions.[3,4] These results have given rise to the proposal that a d^2 hydrazine complex, namely $Cp^*WMe_3(\eta^2\text{-}NH_2NH_2)$, lies on the kinetic pathway to ammonia in this system.[4] Therefore an important goal is to determine how to control the cleavage of the N–N bond in hydrazine to give only ammonia. Hydrazine usually reacts in poorly-defined ways with transition metals in solution to give reduced transition metal complexes that often contain dinitrogen, ammonia, or nitride ligands[6–9] and is known to be decomposed catalytically to ammonia and dinitrogen by transition metals such as chromium and manganese in the presence of acid.[10]

The chemistry of complexes that contain the Cp^*MoMe_3 core has been relatively limited compared to the chemistry of complexes that contain the Cp^*WMe_3 core. For example, Cp^*MoMe_4 can be oxidized at +0.10 V (versus $FeCp_2$), but the oxidation is irreversible, and $[Cp^*MoMe_4]PF_6$ therefore has never been prepared.[11] This result contrasts with the finding that Cp^*WMe_4 can be oxidized to $[Cp^*WMe_4]PF_6$ chemically, and both Cp^*WMe_4 and $[Cp^*WMe_4]^+$ possess well-defined electrochemistry.[12] A second example of the difference between Mo and W is that reduction of $Cp^*MoMe_3(OTf)$ under dinitrogen does not form $[Cp^*MoMe_3]_2(\mu\text{-}N_2)$ or any other identifiable products, even though $[Cp^*MoMe_3]_2(\mu\text{-}N_2)$ has been prepared by other routes.[11] The mechanism of forming $[Cp^*WMe_3]_2(\mu\text{-}N_2)$ is believed to consist of binding of dinitrogen to Cp^*WMe_3, followed by electrophilic attack on N_β in η^1-bound dinitrogen by $Cp^*WMe_3(OTf)$, loss of the triflate ion, and addition of a second electron. Why $[Cp^*MoMe_3]_2(\mu\text{-}N_2)$ cannot be prepared by reducing $Cp^*MoMe_3(OTf)$ under dinitrogen is not known.

In this paper we present the synthesis and some of the chemistry (including N–N bond cleavage studies) of complexes that contain

(1) O'Regan, M. B.; Liu, A. H.; Finch, W. C.; Schrock, R. R.; Davis, W. M. *J. Am. Chem. Soc.* **1990**, *112*, 4331.
(2) Schrock, R. R.; Liu, A. H.; O'Regan, M. B.; Finch, W. C.; Payack, J. F. *Inorg. Chem.* **1988**, *27*, 3574.
(3) Schrock, R. R.; Glassman, T. E.; Vale, M. G. *J. Am. Chem. Soc.* **1991**, *113*, 725.
(4) Schrock, R. R.; Glassman, T. E.; Vale, M. G.; Kol, M. *J. Am. Chem. Soc.* **1993**, *115*, 1760.
(5) Glassman, T. E.; Vale, M. G.; Schrock, R. R. *Organometallics* **1991**, *10*, 4046.
(6) Dilworth, J. R.; Richards, R. L. In *Comprehensive Organometallic Chemistry*; Wilkinson, G., Stone, F. G. A., Abel, E. W., Eds.; Pergamon: London, 1982; Vol. 8, p 1073.
(7) Richards, R. L. *Chem. Br.* **1988**, *24*, 133.
(8) Henderson, R. A.; Leigh, G. J.; Pickett, C. J. *Adv. Inorg. Chem. Radiochem.* **1983**, *27*, 197.
(9) Chatt, J.; Dilworth, J. R.; Richards, R. L. *Chem. Rev.* **1978**, *78*, 589.
(10) Bellerby, J. M. *J. Hazard. Mater.* **1986**, *13*, 57.
(11) Schrock, R. R.; Kolodziej, R. M.; Liu, A. H.; Davis, W. M.; Vale, M. G. *J. Am. Chem. Soc.* **1990**, *112*, 4338.
(12) Liu, A. H.; Murray, R. C.; Dewan, J. C.; Santarsiero, B. D.; Schrock, R. R. *J. Am. Chem. Soc.* **1987**, *109*, 4282.

0020-1669/93/1332-2767$04.00/0

the Cp^*MoMe_3 core. The object is to determine to what extent the chemistry of Cp^*MoMe_3 complexes differs from that of Cp^*WMe_3 complexes and, in particular, whether either Mo or W offers any advantage in terms of N–N bond cleavage to give ammonia.

Results and Discussion

Synthesis and Deprotonation of Mo(V) Hydrazine Complexes. The most straightforward entry into the chemistry of hydrazido complexes that contain the Cp^*WMe_3 core has been addition of hydrazine and methylhydrazines to $Cp^*WMe_3(OTf)$.[4] Addition of N_2H_4, N_2H_3Me, NH_2NMe_2, and NHMeNHMe to $Cp^*MoMe_3(OTf)$ proceeds cleanly to yield complexes of the type $[Cp^*MoMe_3(N_2H_xMe_y)]OTf$ (eq 1). Complexes **1a–1d** are

$$Cp^*MoMe_3(OTf) \xrightarrow[\text{ether}]{N_2H_xMe_y} [Cp^*MoMe_3(N_2H_xMe_y)]OTf \quad (1)$$

1a (N_2H_4), **1b** (N_2H_3Me), **1c** (NH_2NMe_2), **1d** (NHMeNHMe)

isolated as microcrystalline solids in good yield and can be recrystallized from THF. On the basis of the structure of $[Cp^*WMe_3(\eta^2\text{-}NH_2NH_2)]OTf$,[4] we presume that the hydrazines are bound in an η^2 fashion also in **1a–1d**. All are purple except **1c**, a fact that might be taken as evidence that the hydrazine is bound in **1c** in an η^1 manner, rather than an η^2 manner, a proposal that would make some sense for steric reasons.

We have accumulated evidence that $[Cp^*WMe_3(\eta^2\text{-}NH_2NH_2)]OTf$ is deprotonated in THF or ether by NEt_3 or DBU (1,8-diazabicyclo[5.4.0]undec-7-ene) to yield unstable $Cp^*WMe_3(\eta^2\text{-}NHNH_2)$, which then disproportionates to $Cp^*WMe_3(\eta^1\text{-}NNH_2)$, $Cp^*WMe_3(NH)$, and ammonia in high yield.[4] $Cp^*WMe_3(\eta^1\text{-}NNH_2)$ is a relatively stable complex that decomposes slowly via loss of methane in solution and in the solid state at 25 °C over a period of several days to form a trimeric complex;[13] $Cp^*WMe_3(NH)$ is also a stable species.[5] However, addition of NEt_3 or DBU to $[Cp^*MoMe_3(NH_2NH_2)]OTf$ did not yield $Cp^*MoMe_3(NNH_2)$ or $Cp^*MoMe_3(NH)$ (a known compound[5]) or any other inorganic products that we could identify. Attempts to prepare $Cp^*MoMe_3(NNH_2)$ by adding hydrazine to $[Cp^*MoMe_3(O\text{-}2,6\text{-}C_6H_3(i\text{-}Pr)_2)]PF_6$ complexes also failed, even though such reactions yield substituted hydrazido complexes (see below).

In contrast to the above results, attempted deprotonation of cationic Mo(V) adducts that contain methylhydrazine or 1,1-dimethylhydrazine yields $Cp^*MoMe_3(NNMeH)$ (**2a**) or $Cp^*MoMe_3(NNMe_2)$ (**2b**), respectively, in ca. 50% yield (eq 2). We

$$[Cp^*MoMe_3(NH_2NRR')]OTf \xrightarrow[-[Et_3NH]OTf]{NEt_3} Cp^*MoMe_3(NNRR') \quad (2)$$

R = H, R′ = Me (**2a**)
R = R′ = Me (**2b**)

presume that all hydrazido(2–) complexes contain an η^1-hydrazido ligand, virtually the only type found in a circumstance where metal–nitrogen π bonding is possible.[8] One might propose that (e.g.) $Cp^*MoMe_3(NHNMeH)$ disproportionates to $Cp^*MoMe_3(NNMeH)$ and $Cp^*MoMe_3(NH_2NMeH)$ and the latter then decomposes to $Cp^*MoMe_3(NH)$ and methylamine. However, $Cp^*MoMe_3(NH)$ is not observed. Therefore we believe that the reactions shown in eq 2 are related to reactions of some related (methylhydrazido)tungsten complexes in which a hydrogen atom or molecular hydrogen nominally is lost at some stage and the N–N bond remains intact.[4] (See also below.) This type of reaction so far has shown up only for methylhydrazido derivatives of tungsten or molybdenum. Complexes **2a** and **2b** also can be prepared by adding methylhydrazine or 1,1-dimethylhydrazine to $[Cp^*MoMe_3(OAr)]PF_6$ (eq 3). Unfortunately, the pure

$$[Cp^*MoMe_3(OAr)]PF_6 \xrightarrow[-ArOH,\ -Et_3NHPF_6]{\text{(i) } NH_2NRR', \text{(ii) } NEt_3} Cp^*MoMe_3(NNRR') \quad (3)$$

2a or **2b**

product cannot be isolated because of coproduction of a relatively nonvolatile phenol and significant side reactions. Although $Cp^*WMe_3(\eta^1\text{-}NNMeH)$ is stable in solution for days, **2a** decomposes in a matter of hours in solution at 25 °C to give methane and an unidentified product that contains only two Mo–Me groups and no NH proton. The dramatic increase in stability of the monomethyl- or dimethylhydrazido(2–) complexes over as yet unobserved $Cp^*MoMe_3(NNH_2)$ can be ascribed to a steric blocking of methane elimination. We were surprised to find that **2a** decomposes at 40 °C in C_6D_6 in a *first*-order manner with $k = 5.5 \times 10^{-4}$ s^{-1} ($t_{1/2}$ = 21 min).

$Cp^*MoMe_3(NNMeH)$ can be lithiated to yield $Cp^*MoMe_3(NNMeLi)$ (**2c**) (eq 4), a yellow-orange crystalline solid that

$$Cp^*MoMe_3(NNMeH) \xrightarrow[\text{ether, } -40\ ^\circ C]{\text{butyllithium}} Cp^*MoMe_3(NNMeLi) \quad (4)$$

2c

decomposes in the solid state in a matter of hours, even at –40 °C. Similar tungsten complexes, $Cp^*WMe_3(NNHLi)$ and $Cp^*WMe_3(NNLi_2)$, also have been prepared, and they too decompose slowly at 25 °C.[14]

Triethylamine reacts with $[Cp^*MoMe_3(NHMeNHMe)]OTf$ to give $[Cp^*MoMe_3(NMeNMeH)]OTf$ in ca. 50% yield. The details of formation of what is nominally a product formed by loss of a hydrogen atom are unclear. $[Cp^*MoMe_3(NMeNMeH)]OTf$ is the only member of the class of Mo(VI) hydrazido(1–) complexes (see below); several tungsten analogs are easily prepared and well-characterized.[4,13]

Reactions of Mo(VI) Hydrazido(2–) Complexes with Acids. Protonation of a hydrazido(2–) complex to produce a W(VI) cationic hydrazido(1–) complex is an important step in the sequence of proposed steps that results in N–N bond cleavage in the Cp^*WMe_3 system.[4] For example, addition of triflic acid to $Cp^*WMe_3(NNH_2)$ yields structurally-characterized $[Cp^*WMe_3(\eta^2\text{-}NHNH_2)]^+$ as the thermodynamic product; $[Cp^*WMe_3(NNH_3)]^+$ is the proposed kinetic product. $[Cp^*WMe_3(NHNH_2)]X$ is relatively stable in solution when X is a noncoordinating anion such as triflate, but if X^- is Cl^-, then methane is lost readily to yield $Cp^*WMe_2X(NNH_2)$.

Addition of acids to **2a** and **2b** (eq 5; Ph^f = 3,5-$C_6H_3(CF_3)_2$) yielded methane and hydrazido(2–) complexes in all cases. At

$$\underset{\textbf{2a or 2b}}{Cp^*MoMe_3(NNRR')} \xrightarrow[-CH_4]{HX} Cp^*MoMe_2X(NNRR') \quad (5)$$

3a-X; R = H, R′ = Me
3b-X; R = R′ = Me
X = Cl, OTf, BF_4, $B(Ph^f)_4$

this stage, we presume that hydrazido(1–) complexes are formed in this reaction and that methane is lost from them, although the precise mechanism of methane loss is not known. Since the Mo–Me groups in the $Cp^*MoMe_2X(NNRR')$ complexes are equivalent, we presume that these complexes have a roughly square pyramidal geometry analogous to that found for $[Cp^*MoMe_3(NNMe_3)]^+$ (see below) in which X is bound trans to the

(13) Glassman, T. E.; Vale, M. G.; Schrock, R. R. *J. Am. Chem. Soc.* **1992**, *114*, 8098.

(14) Glassman, T. E.; Liu, A. H.; Schrock, R. R. *Inorg. Chem.* **1991**, *30*, 4723.

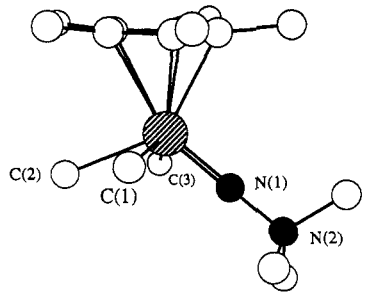

Figure 1. Structure of [Cp*MoMe$_3$(NNMe$_3$)]OTf (anion not shown).

Table I. Relevant Bond Distances (Å) and Bond Angles (deg) for [Cp*MoMe$_3$(NNMe$_3$)]OTf

Mo–N(1)	1.735(4)	N(1)–N(2)	1.426(5)
Mo–C(1)	2.209(5)	N(2)–C(21)	1.503(6)
Mo–C(2)	2.237(6)	N(2)–C(22)	1.488(7)
Mo–C(3)	2.202(6)	N(2)–C(23)	1.494(7)
Mo–N(1)–N(2)	179.2(3)	N(1)–N(2)–C(21)	108.6(4)
N(1)–Mo–C(1)	87.8(2)	N(1)–N(2)–C(22)	108.7(4)
N(1)–Mo–C(2)	117.4(2)	N(1)–N(2)–C(23)	109.1(4)
N(1)–Mo–C(3)	87.6(2)	C(21)–N(2)–C(22)	110.6(4)
C(1)–Mo–C(3)	138.0(2)	C(21)–N(2)–C(23)	109.6(4)
C(1)–Mo–C(2)	72.3(2)	C(22)–N(2)–C(23)	110.3(4)
C(2)–Mo–C(3)	73.1(2)		

imido ligand. Solid-state IR spectra of Cp*MoMe$_2$(OTf)(NNMe$_2$) show a band at 1210 cm^{-1} consistent with a covalently-bound triflate ion. [Cp*WMe$_2$X]$_2$(μ-N$_2$) complexes also are formed upon addition of acids to [Cp*WMe$_3$]$_2$(μ-N$_2$), and two of these complexes have been structurally characterized and shown to contain X trans to nitrogen in what is roughly a square pyramid.[1] The chloride and triflate salts are soluble in ether and are stable indefinitely in solution. The nature of the derivatives that contain "noncoordinating" counterions, BF$_4^-$ and (especially) B(Ph^f)$_4^-$, is less certain. In contrast to the chloride and triflate salts, the BF$_4^-$ and B(Ph^f)$_4^-$ salts are insoluble in ether and decompose in a solvent such as dichloromethane at room temperature over a period of hours. Although examples of BF$_4^-$ binding to a metal are now numerous,[15,16] the possibility of the B(Ph^f)$_4^-$ ion binding to the metal would seem to be remote. Methane is not formed when BF$_4^-$ and PF$_6^-$ ions are employed in the tungsten system.[2,13]

Synthesis and X-ray Structure of a Mo(VI) Hydrazidium Complex. Protonation of Cp*WMe$_3$(NNH$_2$) was proposed to occur most rapidly at N$_\beta$ to form an unobservable hydrazidium complex, [Cp*WMe$_3$(NNH$_3$)]$^+$, and more slowly, but still rapidly overall, at N$_\alpha$ to yield [Cp*WMe$_3$(η^2-NHNH$_2$)]$^+$ as the thermodynamic product.[13] Hydrazidium complexes (e.g., [Cp*WMe$_3$(NNH$_2$Me)]$^+$ and [Cp*WMe$_3$(NNHMe$_2$)]$^+$) became progressively more stable and observable as more methyl methyl groups were added to N$_\beta$, and methylation of Cp*WMe$_3$(NNH$_2$) in the presence of a base yielded stable [Cp*WMe$_3$(NNMe$_3$)]$^+$. If [Cp*MoMe$_3$(NNH$_2$Me)]$^+$ and [Cp*MoMe$_3$(NNHMe$_2$)]$^+$ are the first products of protonating **2a** and **2b**, they would probably be less stable than the tungsten analogs and not observable. However, addition of MeOTf to Cp*MoMe$_3$(NNMe$_2$) yields [Cp*MoMe$_3$(NNMe$_3$)]$^+$ (**5**, eq 6), whose structure is shown in

$$\text{Cp*MoMe}_3(\text{NNMe}_2) \xrightarrow{\text{MeOTf}} [\text{Cp*MoMe}_3(\text{NNMe}_3)]\text{OTf} \quad (6)$$

5

Figure 1. Relevant bond distances and angles are listed in Table I. **5** is the only monomeric hydrazido(2–)-like complex containing the Cp*MMe$_3$ core (M = Mo, W) to have been structurally characterized.

The structure of [Cp*MoMe$_3$(NNMe$_3$)]$^+$ is approximately a square pyramid. The Mo–N(1) bond distance (1.735(4) Å) is relatively short and the Mo–N(1)–N(2) angle is essentially linear (179.2(3)°), both characteristic of sp hybridization at N$_\alpha$ and formation of two π bonds to the metal; in this case the two π bonds are formed using the $\pi_\parallel$ orbital (ca. 65% d_{xy} in the Cp*WMe$_3$ core[4]) and the $\pi_\perp$ orbital (ca. 50% d_{z^2} in the Cp*WMe$_3$ core[4]). (The z axis is taken to be perpendicular to the plane of the Cp* ligand.) The fact that the C(2)–Mo–N(1) angle (117.4(2)°) is significantly smaller than the C(1)–Mo–C(3) angle (138.0(2)°)—N$_\alpha$ of the hydrazidium ligand is displaced below the ideal position in a square pyramid—is also indicative of a π bond being formed between both the $\pi_\parallel$ orbital and $\pi_\perp$ orbitals. The N(1)–N(2) bond distance (1.426(5) Å) is what would be expected for a N–N single bond. The methyl groups cis to N$_\alpha$ are bent away from N$_\alpha$ to a significant extent (N(1)–Mo–C(1) = 87.8(2)°; N(1)–Mo–C(3) = 87.6(2)°) toward C(2) (C(1)–Mo–C(2) = 72.3(2)°; C(2)–Mo–C(3) = 73.1(2)°). All of these features of the central Cp*MoMe$_3$(N) core are similar to those found in ditungsten or dimolybdenum hydrazido(4–) complexes such as [Cp*MoMe$_3$]$_2$(μ-N$_2$),[1,11] the exception being that the M–N bond lengths are generally much longer in the hydrazido(4–) complexes (ca. 1.82 Å) than in the Mo hydrazidium complex, consistent with a significant degree of conjugation in the M=N—N=M system and consequently a weaker M—N pseudo triple bond. There is no feature of the hydrazidium ligand in this high-oxidation-state complex that sets it apart from hydrazidium ligands bound to lower-oxidation-state Mo or W centers,[7-9,17] including the parent hydrazidium ligand itself in [W(PMe$_3$)$_4$Cl(NNH$_3$)]Cl$_2$.[18,19]

It has been proposed that the hydrazidium complex is an important intermediate in a reaction in which an N–N bond is cleaved in many low-oxidation-state Mo or W complexes.[7-9,17] However, [W(PMe$_3$)$_4$Cl(NNH$_3$)]Cl$_2$, for example, does not undergo N–N bond cleavage under the conditions typically employed in that type of chemistry.[19] It is interesting to note that the N–N bond in [Cp*MoMe$_3$(NNMe$_3$)]OTf also is not cleaved under a variety of conditions sufficient to cleave the N–N bond in related Cp*MoMe$_3$(hydrazido) complexes (see below). The only product of reducing [Cp*MoMe$_3$(NNMe$_3$)]OTf with zinc amalgam or cobaltocene that we could identify is Cp*MoMe$_3$(NNMe$_2$). This result could be taken as further evidence that hydrazidium complexes are *not* intermediates on the most facile N–N bond cleavage reaction pathway.

Stoichiometric Reductions. We have found that reduction of homo- and heterobimetallic hydrazido(4–) complexes containing the Cp*MMe$_3$ core (M = Mo, W) is best explained by a mechanism whose first step consists of hydrolysis of one end of the hydrazido(4–) ligand to give an η^1-hydrazido(2–) complex.[11] We also have shown that Cp*WMe$_3$(NNH$_2$) and [Cp*WMe$_3$(η^2-NH$_2$NH$_2$)]$^+$ are reduced efficiently to yield almost 2 equiv of ammonia.[4] Therefore we believe that cleavage of the N–N bond at a single metal center is most likely the most efficient in the Cp*WMe$_3$ system and have proposed that Cp*WMe$_3$(NH$_2$NH$_2$) is the crucial (unobserved) intermediate in which the N–N bond is cleaved.[4] Reduction studies typically employed zinc amalgam as the reducing agent and 2,6-lutidine hydrochloride as the proton source in THF.

Cp*MoMe$_3$ complexes were reduced under conditions similar to those used to reduce tungsten complexes.[4] The results are shown in Table II. Three tungsten complexes are included for the sake of comparison. An important finding is that [Cp*-

(15) Brown, D. H.; Nuttall, R. H.; McAvoy, J.; Sharp, D. W. A. *J. Chem. Soc. A* **1966**, 892.
(16) Mayfield, H. G.; Bull, W. E. *J. Chem. Soc. A* **1971**, 2279.
(17) Barclay, J. E.; Hills, A.; Hughes, D. L.; Leigh, G. J.; Macdonald, C. J. *J. Chem. Soc., Dalton Trans.* **1990**, 2503.
(18) Galindo, A.; Hills, A.; Hughes, D. L.; Richards, R. L. *J. Chem. Soc., Chem. Commun.* **1987**, 1815.
(19) Galindo, A.; Hills, A.; Hughes, D. L.; Richards, R. L.; Hughes, M.; Mason, J. *J. Chem. Soc., Dalton Trans.* **1990**, 283.

Table II. Ammonia Production in THF Using Zinc Amalgam as the Reductant and 2,6-Lutidine Hydrochloride as the Proton Source[a]

complex	ammonia yield (equiv)	% of theory[b]
$Cp^*MoMe_3(NNMe_2)$	0.65	64(2)
$Cp^*WMe_3(NNMe_2)$	0.65	65(3)
$Cp^*MoMe_3(NNMeH)$	0.62	62(2)
$[Cp^*MoMe_3(N_2H_4)]OTf$	1.84	92(2)[c]
$[Cp^*WMe_3(\eta^2\text{-}N_2H_4)]OTf$	1.82	91(1)[d]
$Cp^*WMe_3(NNH_2)$	1.84	92(2)[c,d]
$Cp^*MoMe_3(OTf)$	0.06	3(1)
N_2H_4	0.06	3(1)

[a] See Experimental Section for conditions. [b] Unless otherwise noted, each study was conducted three times, the range (±) is shown in parentheses. [c] Study was conducted six times. [d] See ref 4.

Table III. Ammonia Formation from $[Cp^*MoMe_3(N_2H_4)]^+$ under Different Conditions[a]

reductant	proton source	% yield[b]
Cp_2Co	lut·HCl	92(2)
Zn/Hg	lut·HCl	92(2)[c]
$SnCl_2$	lut·HCl	62(3)
Zn/Hg	phenol	69(3)
Zn/Hg	H_2	65(3)

[a] See Experimental Section for conditions. [b] Unless otherwise noted, each study was conducted three times; the range (±) is shown in parentheses. [c] Study was conducted six times.

$MoMe_3(NH_2NH_2)]^+$ is reduced as efficiently as $[Cp^*WMe_3(\eta^2\text{-}NH_2NH_2)]^+$. Unfortunately, $Cp^*MoMe_3(NNH_2)$ is not available, so we could only explore the reduction of monomethyl- and dimethylhydrazido(2-) species. Only about 65% of the possible 1 equiv of ammonia was formed from **2a** and **2b**, but the same is true in the case of $Cp^*WMe_3(NNMe_2)$. Therefore, again there is virtually no difference between Mo and W complexes as far as the yield of ammonia is concerned. We did not expect to be able to reduce dinitrogen itself starting with $Cp^*MoMe_3(OTf)$, and indeed very little ammonia was detected (ca. 3%). Hydrazine itself, in the absence of any metal complex, is reduced by 12 equiv of Zn/Hg or Cp_2Co in the presence of 16 equiv of lut·HCl to give only traces (ca. 3%) of ammonia.

The reduction of $[Cp^*MoMe_3(NH_2NH_2)]^+$ was carried out using several different combinations of reducing agent and proton source (Table III). Cobaltocene was found to be a successful reducing agent, but $SnCl_2$ was not. ($SnCl_2$ has been used as a reducing agent in dinitrogen chemistry of lower-oxidation-state metals.[20]) Phenol and dihydrogen were found to be relatively inefficient proton sources compared to lutidine hydrochloride.

Catalytic Reduction of Hydrazine. Hydrazine can be reduced catalytically to ammonia by tungsten Cp^*WMe_3 complexes under the same conditions that the N–N bond is cleaved in hydrazine and hydrazido complexes.[4] $Cp^*WMe_3(NH_2NH_2)$ again is proposed to be the crucial intermediate in which the N–N bond is cleaved. The reaction shown in eq 7 has been demonstrated

$$Cp^*WMe_3(NH_2) \underset{-NH_3}{\overset{+N_2H_4}{\rightarrow}} Cp^*WMe_3(NHNH_2) \qquad (7)$$

and is believed to be a step in the catalytic reduction sequence. In the absence of protons, $Cp^*WMe_3(NHNH_2)$ disproportionates to $Cp^*WMe_3(NH_2NH_2)$ and $Cp^*WMe_3(NH)$ (plus ammonia), but in the presence of protons, $Cp^*WMe_3(NHNH_2)$ is believed to be protonated to yield $[Cp^*WMe_3(NH_2NH_2)]^+$. The complete proposed sequence for the reduction of hydrazine is shown in Scheme I.

Hydrazine can be reduced catalytically also by $[Cp^*MoMe_3(N_2H_4)]OTf$. The yields of ammonia (Table IV) range from 95% to 81% (for 6 equiv of hydrazine). (It should be noted that the maximum possible yield of ammonia via disproportionation of hydrazine to ammonia and molecular nitrogen is 67%.) Zinc amalgam and lutidinium chloride were employed in THF at 25 °C over a period of 16–28 h. The decrease in the yield of ammonia as the number of equivalents of hydrazine increases also was observed by employing $[Cp^*WMe_3(\eta^2\text{-}N_2H_4)]OTf$ as the catalyst, where only 72% of the theoretical amount of ammonia was produced from 10 equiv of hydrazine.[4] We assume either that the catalyst degrades in the presence of increasing amounts of hydrazine or that disproportionation of hydrazine to ammonia and molecular nitrogen becomes the dominant reaction with time. It should be noted that the yields of ammonia with $[Cp^*MoMe_3(N_2H_4)]OTf$ as the catalyst are virtually identical to the yields with $[Cp^*WMe_3(\eta^2\text{-}N_2H_4)]OTf$ as the catalyst[4] and that the catalytic cycle (Scheme I) does not involve $[Cp^*MoMe_3(NHNH_2)]^+$, an unobservable and (proposed) unstable species.

Scheme I. Proposed Mechanism for Reduction of Hydrazine to Ammonia by Cp^*MMe_3 Complexes

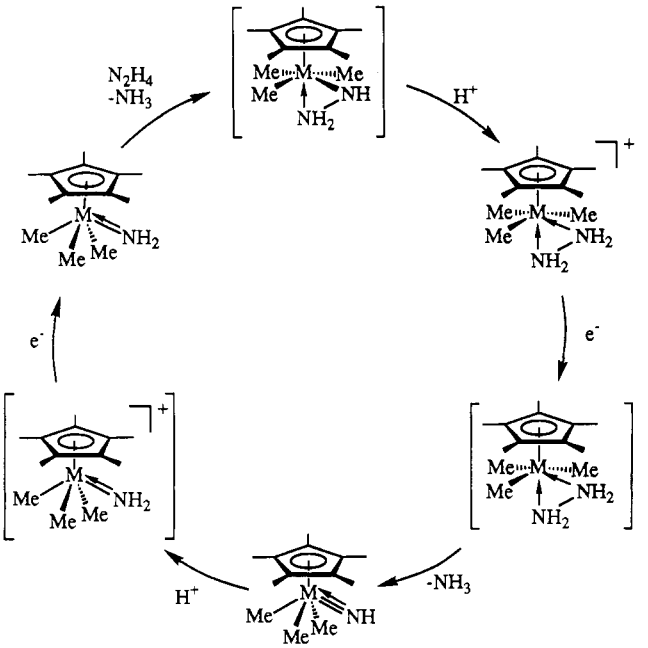

Table IV. Catalytic Reduction of Hydrazine to Ammonia Using $[Cp^*MoMe_3(N_2H_4)]^+$ [a]

amt of N_2H_4 (equiv)	NH_3 yield (equiv)	% yield[b]
0	1.86	92(2)[c]
2	5.70	95(3)
3	6.88	87(2)
4	8.70	84(2)
6	11.62	81(3)

[a] See Experimental Section for conditions. [b] Unless otherwise noted, each study was conducted three times; the range (±) is shown in parentheses. [c] Study was conducted six times.

Conclusion

The central theme of the results presented here is that while much of the chemistry of the Cp^*MoMe_3 core is analogous to that involving the Cp^*WMe_3 core, the chemistry of the Mo system is not as well-defined or controlled as the W system, perhaps primarily because of relatively rapid side reactions, among them loss of a methyl group to give methane. On the other hand, many of the steps that are necessary for the controlled cleavage of the N–N bond to give 2 equiv of ammonia are as successful in the Mo system as in the W system, as is the catalytic reduction of hydrazine. Therefore there seems to be no significant advantage or disadvantage in principle to using Mo or W for N–N reduction beyond the hydrazido(2-) stage. A characteristic of Cp^*MMe_3 centers that is potentially of general significance for reducing N_2H_x species is the presence of two π orbitals and one σ orbital that are used to bind a variety of N_2H_x ligands. Ultimately it would seem desirable to design other ligand systems that have

(20) George, T. A.; Kaul, B. B. *Inorg. Chem.* **1991**, *30*, 882.

the $2\pi,1\sigma$ combination of bonding orbitals, especially systems that are resistant to degradation by protons and that are sterically protected against bimolecular reactions. Experiments aimed in this direction are in progress.

Experimental Section

General Information. Solvents were dried and degassed prior to use and distilled from molten sodium (toluene), sodium/benzophenone (diethyl ether, tetrahydrofuran, pentane), CaH_2 (dichloromethane), or P_2O_5 (acetonitrile). Pentane was washed with 5% HNO_3/H_2SO_4 and dried using tetraglyme to solvate the sodium. All preparations were conducted under a nitrogen atmosphere in a Vacuum Atmospheres drybox, under argon in Schlenkware, or on a high-vacuum line ($<10^{-4}$ Torr). Triflic acid was purchased from Aldrich and used directly from the sealed ampule.

NMR operating frequencies and reference standards are as follows: ^{1}H, 300.1 MHz, $SiMe_4$ = 0 ppm; ^{13}C, 75.0 MHz, $SiMe_4$ = 0 ppm; ^{15}N, 30.4 MHz, NH_2Ph = 56.5 ppm; ^{19}F, 282.2 MHz, $CFCl_3$ = 0 ppm. Proton and carbon NMR data were referenced using resonances for the partially deuterated NMR solvent. Other nuclei were referenced externally in the same solvent unless otherwise noted. Chemical shifts are in ppm, and coupling constants and line widths are in hertz. All spectra were acquired at room temperature unless otherwise noted. Deuterated solvents were dried by passage through alumina and storage over 4-Å molecular sieves. IR spectra were acquired on a Mattson Cygnus 100 FT-IR spectrometer for samples in Nujol mulls between KBr plates unless otherwise indicated. ESR spectra were obtained on a Bruker ESP 300 spectrometer in 3-mm quartz tubes in dichloromethane at room temperature unless otherwise noted; the line width ($\Delta\nu_{1/2}$) is given in parentheses. Microanalyses (C, H, and N) were performed in our laboratory using a Perkin-Elmer PE2400 microanalyzer.

Methyl- and dimethylhydrazines were dried as liquids under pressure over sodium and distilled. 1,8-Diazabicyclo[5.4.0]undec-7-ene (DBU) was purchased from Aldrich. Cp*MoMe$_3$(OTf)[11] and HB[3,5-C_6H_3-$(CF_3)_2]_4$[21] were prepared as reported in the literature.

Preparation of Compounds. [Cp*MoMe$_3$(N_2H_4)]OTf (1a). Hydrazine (0.015 mL, 0.470 mmol) was added to a solution of Cp*MoMe$_3$(OTf) (0.200 g, 0.470 mmol) in 15 mL of cold (−30 °C) ether. A purple precipitate appeared within 30 s. After 5 min, purple [Cp*MoMe$_3$-(N_2H_4)]OTf (0.150 g, 0.328 mmol, 70%) was filtered off: ESR $\langle g\rangle$ = 2.012, A_{Mo} = 47 G, $\Delta\nu_{1/2}$ = 34 G; IR (Nujol, cm^{-1}) 3325 (s, NH stretch), 3237 (s, NH stretch), 3109 (s, NH stretch), 1590 (s, NH bend), 1570 (s, NH bend). Anal. Calcd for $C_{14}H_{28}N_2S_3F_3Mo$: C, 36.76; H, 6.17; N, 6.12. Found: C, 36.37; H, 6.08; N, 6.06.

[Cp*MoMe$_3$(NH_2NHMe)]OTf (1b). As in the synthesis of **1a**, addition of N_2H_3Me (0.038 mL, 0.705 mmol) to Cp*MoMe$_3$(OTf) (0.300 g, 0.705 mmol) in 10 mL of ether yielded [Cp*MoMe$_3$(N_2H_3Me)]OTf as a purple solid (0.225 g, 0.477 mmol, 68%): ESR $\langle g\rangle$ = 2.008, A_{Mo} = 26 G, $\Delta\nu_{1/2}$ = 26 G; IR (Nujol, cm^{-1}) 3314, 3170 (NH stretch), 1735, 1617 (NH bend). Anal. Calcd for $MoC_{15}H_{27}N_2SO_3F_3$: C, 38.22; H, 6.41; N, 5.94. Found: C, 38.40; H, 6.47; N, 5.94.

[Cp*MoMe$_3$(NH_2NMe$_2$)]OTf (1c). As in the synthesis of **1a**, addition of NH_2NMe_2 (0.054 mL, 0.705 mmol) to Cp*MoMe$_3$(OTf) (0.300 g, 0.705 mmol) yielded [Cp*MoMe$_3$(NH_2NMe$_2$)]OTf as a tan solid (0.220 g, 0.453 mmol, 64%): ESR $\langle g\rangle$ = 2.004, A_{Mo} = 20 G, $\Delta\nu_{1/2}$ = 28 G; IR (Nujol, cm^{-1}) 3280, 3180 (NH stretch), 1746, 1670 cm^{-1} (NH bend).

[Cp*MoMe$_3$(1,2-N_2H_2Me$_2$)]OTf (1d). As in the synthesis of **1a**, addition of 1,2-$N_2H_2Me_2$ (0.376 mL of 1.25 M solution in ether, 0.470 mmol) to Cp*MoMe$_3$(OTf) (0.200 g, 0.470 mmol) dissolved in 30 mL of cold ether (−30 °C) yielded [Cp*MoMe$_3$(1,2-$N_2H_2Me_2$)]OTf as a light purple solid (0.166 g, 0.342 mmol, 73%): ESR $\langle g\rangle$ = 2.004, A_{Mo} = 22 G; $\Delta\nu_{1/2}$ = 25 G; IR (Nujol, cm^{-1}) 3220 (m, NH stretch), 3140 (s, NH stretch), 1250 (s, OTf), 1027 (s), 619 (s).

Cp*MoMe$_3$(NNMeH) (2a). [Cp*MoMe$_3$(NH_2NHMe)]OTf (0.500 g, 1.061 mmol) was suspended in 50 mL of cold ether (−30 °C), and NEt_3 (0.444 mL, 3.182 mmol) was added. The reaction mixture was stirred for 1 h and filtered. The solvent was removed from the yellow-brown filtrate in vacuo to give a yellow-orange solid, which was extracted with pentane. The yellow-orange extract was filtered, and the solvent was removed to leave yellow Cp*MoMe$_3$(NNMeH) (0.167 g, 0.520 mmol, 49%): ^{1}H NMR (C_6D_6) δ 5.19 (br, 1, NMe*H*), 2.30 (d, 3, N*Me*H), 1.57 (s, 15, Cp*), 0.84 (s, 6, Mo–Me_c), 0.43 (s, 3, Mo–Me_t); ^{13}C NMR (C_6D_6) δ 108.2 (s, Me_5C_5), 36.8 (q, NN*Me*H), 29.6 (q, Mo-Me_c), 22.7 (q, Mo-Me_t), 10.2 (q, Me_5C_5); IR (Nujol, cm^{-1}) 892 (Mo=N). Anal. Calcd for $C_{14}H_{28}N_2Mo$: C, 52.49; H, 8.81; N, 8.75. Found: C, 52.58; H, 8.97; N, 8.57.

Cp*MoMe$_3$(NNMe$_2$) (2b). This was prepared by a route similar to that described above for **2a** starting with [Cp*MoMe$_3$(NH_2NMe$_2$)]OTf (0.500 g, 1.030 mmol): yield 0.171 g (0.514 mmol, 50%); ^{1}H NMR (C_6D_6) δ 2.45 (s, 6, NMe_2), 1.60 (s, 15, Cp*), 0.88 (s, 6 , Mo–Me_c), 0.40 (s, 3, Mo–Me_t); ^{13}C NMR (C_6D_6) δ 107.2 (s, Me_5C_5), 35.3 (q, NMe_2), 28.3 (q, Mo–Me_c), 21.8 (q, Mo–Me_t), 10.4 (q, Me_5C_5); IR (Nujol, cm^{-1}) 889 (Mo=N). Anal. Calcd for $C_{15}H_{30}N_2Mo$: C, 53.88; H, 9.04; N, 8.38. Found: C, 53.73; H, 8.76; N, 8.37.

Cp*MoMe$_3$(NNMeLi) (2c). Cp*MoMe$_3$(NNMeH) (0.072 g, 0.225 mmol) was dissolved in 10 mL of ether at −40 °C, 2.5 M *n*-BuLi (0.112 mL, 0.225 mmol) was added, and the mixture was stirred for 20 min. A yellow precipitate formed. The reaction mixture was cooled to −40 °C and filtered to give Cp*MoMe$_3$(NNMeLi) (0.065 g, 0.199 mmol, 89%) as a yellow-orange solid: ^{1}H NMR (THF-d_8) δ 3.10 (br s, 3, NNMeLi), 1.69 (s, 15, Cp*), −0.20 (s, 6, Mo–Me_c), −0.82 (s, 3, Mo–Me_t); ^{13}C NMR (THF-d_8) δ 104.1 (s, C_5Me_5), 42.6 (q, NNMeLi), 23.7 (q, Mo–Me_t), 18.7 (q, Mo–Me_c), 11.5 (C_5Me_5). Anal. Calcd for $MoC_{14}H_{27}N_2Li$: C, 51.54; H, 8.34; N, 8.59. Found: C, 51.77; H, 8.14; N, 8.35.

Cp*MoMe$_2$Cl(NNMeH) (3a-Cl). Cp*MoMe$_3$(NNMeH) (0.175 g, 0.543 mmol) was dissolved in 10 mL of ether at −40 °C. An ethereal solution of HCl (0.159 g, 0.156 mmol) was added directly to the stirred solution. The reaction mixture turned a cloudy light yellow color immediately. After 20 min, the mixture was filtered to yield a small quantity (<5 mg) of a white solid and a yellow filtrate. The solvent was removed from the filtrate in vacuo to produce a green-yellow solid, which was washed with pentane, dried, and collected: yield 0.096 g (0.283 mmol, 52%); ^{1}H NMR (CD_2Cl_2) δ 6.90 (br s, 1, NMe*H*), 3.10 (d, 3, N*Me*H), 1.60 (s, 15, Cp*), 1.30 (s, 6, Mo–Me); ^{13}C NMR (CD_2Cl_2) δ 117.9 (s, Me_5C_5), 59.1 (q, N*Me*H), 37.6 (q, Mo–Me), 10.7 (q, Me_5C_5). Anal. Calcd for $MoC_{13}H_{24}N_2Cl$: C, 45.96; H, 7.12; N, 8.25. Found: C, 45.61; H, 7.35; N, 7.90.

Cp*MoMe$_2$(OTf)(NNMeH) (3a-OTf). Cp*MoMe$_3$(NNMeH) (0.068 g, 0.212 mmol) was dissolved in 8 mL of ether at −40 °C. HOTf (18.8 μL, 0.212 mmol) dissolved in 2 mL of ether was added via a cold pipet to the stirred solution. The cloudy orange-yellow solution was stirred for 1 min and then stored at −40 °C for 30 min. A yellow solid precipitated from the solution. The solvent was decanted, and the solid was washed with pentane. Orange Cp*MoMe$_2$(OTf)(NNMeH) was collected (0.070 g, 0.154 mmol, 73%): ^{1}H NMR (CD_2Cl_2) δ 9.15 (s, 1, NMe*H*), 3.42 (s, 3, N*Me*H), 1.93 (s, 15, Cp*), 1.40 (s, 6, Mo–Me); ^{13}C NMR (CD_2Cl_2) δ 118.5 (s, Me_5C_5), 59.4 (q, N*Me*H), 40.2 (q, Mo–Me), 13.7 (q, Me_5C_5); ^{19}F NMR (CD_2Cl_2) δ −78.89 (s, OSO_2CF_3). Anal. Calcd for $MoC_{14}H_{25}N_2SO_3F_3$: C, 37.01; H, 5.55; N, 6.17. Found: C, 37.04; H, 5.44; N, 5.77.

Cp*MoMe$_2$(BF$_4$)(NNMeH) (3a-BF$_4$). Cp*MoMe$_3$(NNMeH) (0.102 g, 0.318 mmol) was dissolved in 8 mL of ether at −40 °C. HBF_4·OMe_2 (0.052 g, 0.318 mmol) dissolved in 2 mL of −40 °C ether was added via a cold pipet to the stirred solution. A light purple solid formed rapidly. The reaction mixture was stirred for 3 min, cooled to −40 °C, and filtered to produce a dark orange-brown filtrate and light purple Cp*MoMe$_2$-(BF_4)(NNMeH) (0.110 g, 0.281 mmol, 88%): ^{1}H NMR (CD_2Cl_2) δ 8.80 (br s, 1, NMe*H*), 3.45 (d, 3, N*Me*H), 1.90 (s, 15, Cp*), 1.57 (s, 6, Mo–Me); ^{13}C NMR (CD_2Cl_2) δ 116.1 (s, Me_5C_5), 57.6 (q, NN*Me*H), 37.1 (q, Mo–Me_t), 10.7 (q, Me_5C_5); ^{19}F NMR (CD_2Cl_2) δ −149.6 (br s, BF_4); FT-IR (Nujol, cm^{-1}) 3261 (m, NH), 1071 (s, BF_4), 882 (s). Anal. Calcd for $MoC_{13}H_{25}N_2BF_4$: C, 39.82; H, 6.43; N, 7.14. Found: C, 39.54; H, 6.56; N, 6.44.

Cp*MoMe$_2$(BPh$^f_4$)(NNMeH) (3a-BPh$^f_4$). Cp*MoMe$_3$(NNMeH) (0.050 g, 0.156 mmol) was dissolved in 10 mL of ether at −40 °C. $HBPh^f_4$·$2Et_2O$ (0.159 g, 0.156 mmol) was added directly to the stirred solution. After 20 min, the reaction mixture was a dark purple-red. The solvent was removed in vacuo to produce purple solid, which was washed with pentane. The purple Cp*MoMe$_2$(BPh$^f_4$)(NNMeH) (0.096 g, 0.081 mmol, 52%) was dried and collected: ^{1}H NMR (CD_2Cl_2) δ 7.42 (s, 8, Ph^f), 7.30 (s, 4, Ph^f), 6.90 (br s, 1, NMe*H*), 3.10 (d, 3, N*Me*H), 1.60 (s, 15, Cp*), 1.30 (s, 6, Mo–Me); ^{13}C NMR (CD_2Cl_2) δ 162.2 (q, CF_3, J_{CF} = 49.8 Hz), 135.2 (d, aryl C), 129.3 (q, aryl C_{ipso}, J_{BC} = 31.5 Hz), 126.8 (s, aryl C_m), 123.2 (s, aryl C_m), 117.9 (s, Me_5C_5), 117.2 (d, aryl C), 59.1 (q, N*Me*H), 37.6 (q, Mo–*Me*), 10.7 (q, Me_5C_5). Anal. Calcd for $MoC_{45}H_{37}N_2BF_{24}$: C, 46.25; H, 3.19; N, 2.40. Found: C, 46.25; H, 3.15; N, 2.37.

Cp*MoMe$_2$Cl(NNMe$_2$) (3b-Cl). Cp*MoMe$_3$(NNMe$_2$) (0.040 g, 0.120 mmol) was dissolved in 10 mL of ether at −40 °C, and 2.87 M HCl (0.042 mL, 0.120 mmol) was added directly to the stirred solution. The

(21) Brookhart, M.; Grant, B.; Volpe, A. F., Jr. *Organometallics* **1992**, *11*, 3920.

reaction mixture turned dark orange and was stirred for 30 min. The solvent was removed in vacuo to give a light green solid. The solid was washed with pentane, and $Cp^*MoMe_2Cl(NNMe_2)$ (0.037 g, 0.105 mmol, 87%) was isolated as a light green solid: ^1H NMR (CD_2Cl_2) δ 3.58 (s, 6, NMe_2), 1.93 (s, 15, Cp*), 1.57 (s, 6, Mo–Me); ^{13}C NMR (C_6D_6) δ 116.6 (s, Me_5C_5), 42.9 (q, NMe_2), 12.4 (q, Mo–Me_t), 11.3 (q, Me_5C_5). Anal. Calcd for $MoC_{14}H_{27}N_2Cl$: C, 47.40; H, 7.67; N, 7.90. Found: C, 47.09; H, 7.43; N, 7.62.

$Cp^*MoMe_2(OTf)(NNMe_2)$ (3b-OTf). $Cp^*MoMe_3(NNMe_2)$ (0.051 g, 0.150 mmol) was dissolved in 8 mL of ether at –40 °C. A solution of HOTf (13.2 μL, 0.150 mmol) in 2 mL of ether was added dropwise to the stirred solution. The reaction was stirred for 2 min and cooled to –40 °C. After 30 min, the solvent was removed in vacuo to produce an orange solid, which was washed with pentane. $Cp^*MoMe_2(OTf)(NNMe_2)$ was collected (0.041 g, 0.136 mmol, 87%) as an orange semicrystalline solid: ^1H NMR (C_6D_6) δ 2.49 (s, 6, NMe_2), 1.45 (s, 15, Cp*), 1.09 (s, 6, Mo–Me); ^{13}C NMR (C_6D_6) δ 114.2 (s, Me_5C_5), 43.2 (q, NMe_2), 31.9 (q, Mo–Me_t), 11.6 (q, Me_5C_5); ^{19}F NMR (C_6D_6) δ –82.8 (s, OSO_2CF_3); IR (Nujol, cm^{-1}) 1209 (m, OTf), 1025 (s), 888 (m), 627 (s, OTf). Anal. Calcd for $MoC_{15}H_{27}N_2SO_3F_3$: C, 38.47; H, 5.81; N, 5.98. Found: C, 38.03; H, 5.81; N, 5.77.

$Cp^*MoMe_2(BF_4)(NNMe_2)$ (3b-BF_4). $Cp^*MoMe_3(NNMe_2)$ (0.055 g, 0.165 mmol) was dissolved in 8 mL of ether at –40 °C. A solution of $HBF_4{\cdot}OMe_2$ (0.015 g, 0.110 mmol) in 2 mL of ether was added dropwise to the stirred solution. A light purple solid formed instantly. After 3 min, the mixture was filtered to yield $Cp^*MoMe_2(BF_4)(NNMe_2)$ (0.058 g, 0.144 mmol, 87%) as a purple solid: ^1H NMR (CD_2Cl_2) δ 3.58 (s, 6, $NNMe_2$), 1.93 (s, 15, Cp*), 1.57 (s, 6, Mo–Me); ^{13}C NMR (C_6D_6) δ 116.6 (s, Me_5C_5), 42.9 (q, $NNMe_2$), 12.4 (q, Mo–Me_t), 11.3 ppm (q, Me_5C_5); ^{19}F NMR (C_6D_6) δ –154.2 (s, BF_4); IR (Nujol, cm^{-1}) 1378 (s), 1049 (s), 882 (s).

$Cp^*MoMe_2(BPh'_4)(NNMe_2)$ (3b-BPh'_4). $Cp^*MoMe_3(NNMe_2)$ (0.050 g, 0.150 mmol) was dissolved in 10 mL of ether at –40 °C. $HB(Ph')_4{\cdot}Et_2O$ (0.152 g, 0.150 mmol) was added directly to the stirred solution. After 15 min, the solvent was removed from the reaction in vacuo and the residue was washed with pentane. $Cp^*MoMe_2(BPh'_4)(NNMe_2)$ was isolated as a purple solid (0.80 g, 0.063 mmol, 45%): ^1H NMR (CD_2Cl_2) δ 3.58 (s, 6, NMe_2), 1.93 (s, 15, Cp*), 1.57 (s, 6, 2 Mo–Me); ^{13}C NMR (C_6D_6) δ 162.3 (q, CF_3, J_{CF} = 49.5 Hz), 135.3 (d, aryl C), 129.5 (q, aryl C_{ipso}, J_{BC} = 32.3 Hz), 126.9 (s, aryl C_m), 123.3 (s, aryl C_m), 118.0 (d, aryl C), 116.6 (s, Me_5C_5), 43.7 (q, $NNMe_2$), 21.7 (q, Mo–Me), 11.1 (q, Me_5C_5). Anal. Calcd for $MoC_{46}H_{39}N_2BF_{24}$: C, 46.72; H, 3.32; N, 2.37. Found: C, 46.31; H, 3.18; N, 1.93.

$[Cp^*MoMe_3(NMeNMeH)]OTf$. $[Cp^*MoMe_3(1,2\text{-}N_2H_2Me_2)]OTf$ (0.165 g, 0.340 mmol) was dissolved in 30 mL of cold (–40 °C) THF. NEt_3 (0.142 mL, 1.012 mmol) was added directly to the stirred solution. The reaction mixture turned yellow-brown. After 30 min, the solvent was removed in vacuo. The yellow-brown residue was extracted with ether and $[Cp^*MoMe_3(NMeNMeH)]OTf$ was filtered off and dried in vacuo (0.078 g, 0.161 mol, 47%): ^1H NMR (CD_2Cl_2) δ 5.85 (br s, 1, NMe*H*), 3.45 (s, 3, NMe), 2.75 (d, 3, N*Me*H), 1.75 (s, 15, Cp*), 0.65 (s, 3, Mo–Me), 0.60 (s, 3, Mo–Me), 0.38 (s, 3, Mo–Me); ^{13}C (CD_2Cl_2) δ 116.2 (s, C_5Me_5), 42.6 (q, $N_\alpha Me$), 42.2 (q, $N_\beta MeH$), 34.0 (q, Mo–Me), 33.2 (q, Mo–Me), 26.7 (q, Mo–Me), 10.9 (q, C_5Me_5). Anal. Calcd for $MoC_{16}H_{31}N_2SO_3F_3$: C, 39.67; H, 6.45; N, 5.57. Found: C, 38.98; H, 6.38; N, 5.93.

$[Cp^*MoMe_3(NNMe_3)]OTf$. Addition of MeOTf (0.020 mL, 0.179 mmol) directly to the stirred solution of $Cp^*MoMe_3(NNMe_2)$ (0.050 g, 0.150 mmol) in 15 mL of cold (–40 °C) ether produced a white precipitate within 2 min. After 1 h, white $[Cp^*Mo^*Me_3(NNMe_3)]OTf$ (0.61 g, 0.121 mmol, 81%) was filtered off: ^1H NMR (CD_2Cl_2) δ 3.50 (s, 9, $NNMe_3$), 1.83 (s, 15, Cp*), 0.91 (s, 6, Mo–Me_c), 0.10 (s, 3, Mo–Me_t); ^{13}C NMR (CD_2Cl_2) δ 113.5 (s, Me_5C_5), 58.4 (q, $NNMe_3$), 32.7 (q, Mo–Me_t), 28.4 (q, Mo–Me_c), 11.2 (q, Me_5C_5); IR (Nujol, cm^{-1}) 940, 805 (Mo=N). Anal. Calcd for $C_{17}H_{33}N_2SO_3F_3Mo$: C, 40.96; H, 6.67; N, 5.62. Found: C, 41.23; H, 6.66; N, 5.63.

X-ray Crystal Structure of $[Cp^*MoMe_3(NNMe_3)]OTf$ (1a). A yellow prism with dimensions 0.28 × 0.28 × 0.24 mm was mounted on a glass fiber. Data were collected at –78 °C on an Enraf-Nonius CAD-4 diffractometer with graphite-monochromated Mo Kα radiation (λ = 0.710 69 Å). A total of 6666 reflections were collected in the range 3.00° < 2θ < 54.90°, with 6315 being unique. No crystal decay was evident during data collection. An empirical absorption correction was applied, using the program DIFABS. The structure was solved using the Patterson method. The non-hydrogen atoms were refined anisotropically. Hydrogen atoms were included in the structure factor calculation in idealized positions. The final cycle of full-matrix least-squares refinement based on 3827 reflections ($I > 3.00\sigma(I)$) and 271 variables used the TEXSAN crystallographic software package from Molecular Structure Corp. The final refinement converged with final R = 0.052 and R_w = 0.051. The maximum and minimum peaks on the final Fourier difference map corresponded to 0.59 and –0.78 e/Å^3, respectively. Crystal data: space group = $P2_1/c$, a = 9.173(1) Å, b = 8.724(3) Å, c = 32.091(6) Å, β = 91.56(2)°, V = 2567(1) Å^3, MW = 583.39, ρ(calcd) = 1.509 g/cm^3, Z = 4, μ = 8.28 cm^{-1}.

Stoichiometric Formation of Ammonia. Method 1. Under an atmosphere of dinitrogen, 30 mg of a given complex was weighed out and added to a 50-mL Schlenk flask. Reductant and proton source were added to the flask (6 and 12 equiv, respectively, in the case of $Cp^*WMe_3(NNH_2)$; 4 and 8 equiv, respectively, in the case of $[Cp^*WMe_3(\eta^2\text{-}N_2H_4)]OTf$), which was then capped with a septum and wired shut. A 10-mL portion of cold (–40 °C) THF was added to the flask via syringe, and the reaction mixture was stirred vigorously. After 20 h at 25 °C, 100 μL of concentrated HCl was added to the reaction mixture by syringe. The solvent was removed in vacuo, and the residue was treated with 15 mL of a 4.0 M NaOH solution in a closed system under argon. The basic solution was then gently distilled into 15 mL of 0.5 N H_2SO_4 until ~10–15 mL of the distillate had been collected. The volume of the acid solution was then brought up to 30 mL with distilled water and ammonia determined quantitatively by the indophenol method.[22]

Method 2. This method differs from method 1 only in the workup of the reaction mixture. After 20 h at 25 °C, 100 μL of concentrated HCl was added to the reaction mixture by syringe. The solvent was then removed in vacuo, and the remaining solids were extracted with 30 mL of distilled water. The extract was then passed through a Millipore filter to remove insoluble solids. Samples of this solution were then tested quantitatively for ammonia by the indophenol method.[22] The yields of ammonia using this method varied only slightly (±3%) from those obtained by method 1.

Catalytic Reduction of Hydrazine. The reaction was set up as described above for the stoichiometric reduction to give ammonia except hydrazine was added. After 20–28 h (depending on the concentration of hydrazine) at 25 °C, 200 μL of concentrated HCl was added to the reaction mixture by syringe. The solvent was then removed in vacuo, and the residue either was treated with 4.0 M NaOH followed by base distillation as described above in method 1 or was extracted with water as described in method 2. Ammonia was determined quantitatively by the indophenol method.[22]

Acknowledgments. R.R.S. thanks the National Institutes of Health for support (Grant GM 31978), and M.G.V. thanks the National Science Foundation for a predoctoral fellowship. We thank Dr. W. M. Davis for collecting X-ray data for **5**.

Supplementary Material Available: A listing of experimental details of the X-ray study of **5**, a labeled ORTEP drawing, and tables of final positional parameters and final thermal parameters (6 pages). Ordering information can be found on any current masthead page.

(22) Chaney, A. L.; Marbach, E. P. *Clin. Chem.* **1962**, *8*, 130.